

A SHOCK TUBE INVESTIGATION OF HEAT TRANSFER FROM DISSOCIATED HYDROGEN TO CATALYTIC SURFACES

A. E. M. NASSER* and R. A. EAST

Department of Aeronautics and Astronautics, University of Southampton,
 SO9 5NH, England

(Received 1 May 1979 and in revised form 29 October 1979)

Abstract – Shock tube experiments are described which compare the heat transfer rate to flat plate nickel and silicon dioxide surfaces from dissociated hydrogen/argon mixtures at temperatures from 2000 to 6000 K. The experimental conditions were chosen in order to permit the effects of surface recombination of hydrogen atoms on the heat-transfer rate to be explored. Comparisons of the experiments with theoretical predictions based on existing laminar boundary layer methods are presented. The results may be interpreted to yield an experimental value for the catalytic efficiency (γ') of silicon dioxide surfaces to hydrogen atom recombination of 25×10^{-4} .

NOMENCLATURE

c , ratio of the density viscosity product, $(\rho\mu/\rho_e\mu_e)$;
 c_f , skin friction coefficient;
 c_p , specific heat at constant pressure;
 h , specific enthalpy;
 h^0 , specific enthalpy of formation at standard reference condition;
 k , Boltzmann's constant;
 k_R , recombination rate constant;
 k_W , surface recombination rate;
 k_D , dissociation rate constant;
 p , pressure;
 \dot{q} , heat-transfer rate;
 w , exponent of temperature in expression $k_R = A/T^w$ (A is a constant);
 x , longitudinal distance from the plate leading edge;
 D , diffusion coefficient;
 D_{12} , binary diffusion coefficient;
 K , thermal conductivity;
 Le , Lewis number, (pDc_p/K) ;
 M , molecular weight;
 Pr , Prandtl number, $(\mu c_p/K)$;
 R , specific gas constant;
 R_0 , universal gas constant;
 Re , Reynolds number, $(\rho_e U_e x/\mu_e)$;
 S , boundary-layer diffusion rate, (equation 2);
 Sc , Schmidt number, (Pr/Le) ;
 St , Stanton number;
 T , temperature;
 U , gas velocity;
 α_A , atom fraction;
 β , energy accommodation coefficient;
 γ' , surface catalytic efficiency;

ϵ , mean depth of the potential well in the Lennard-Jones potential;
 ϵ_{12} , $\sqrt{(\epsilon_1\epsilon_2)}$;
 ϕ , $(1 + S/k_W)^{-1}$;
 ρ , gas density;
 σ , collision diameter [\AA];
 σ_{12} , $(\sigma_1 + \sigma_2)/2$;
 τ_d , characteristic boundary-layer particle diffusion time;
 τ_p , characteristic gas phase reaction time;
 τ_s , characteristic surface reaction time;
 ζ_g , gas phase Damkohler number;
 ζ_s , surface reaction Damkohler number;
 μ , viscosity coefficient;
 $\Omega^{(1,1)*}$, collision integral;
 $\Omega^{(2,2)}$, collision integral.

Subscripts

e , refers to conditions at edge of boundary layer;
 r , recovery values;
 w , refers to conditions at plate surface;
 A , refers to atomic species;
 H , hydrogen atoms;
 T , total or stagnation conditions;
 Ni , nickel;
 SiO_2 , silicon dioxide;
 $1, 2$, refer to different species.

Superscript

$*$, refers to quantities evaluated at intermediate enthalpy conditions.

1. INTRODUCTION

IN CHEMICALLY frozen and non-equilibrium flows metallic surfaces tend to catalyse surface recombination of atomic species, the enthalpy of recombination consequently increasing the surface heat transfer rate in comparison with non-metallic surfaces which have much lower catalytic efficiencies. An

* Present address: Department of Mechanical Engineering, Riyadh University, Saudi Arabia.

example of past work in which this phenomenon is of importance is in the context of the aerodynamic heat transfer to bodies having catalytic or non-catalytic surfaces from high temperature reacting air during atmospheric re-entry.

Renewed interest in this field of study arises from possible applications to combustion systems, firstly, in determining heat transfer from non-equilibrium zones in combustion products, and secondly with relevance to the physical phenomena occurring in non-equilibrium boundary layers adjacent to catalytic surfaces promoting catalytic combustion. In the former problem, diffusion and subsequent surface recombination of atomic species and radicals can result in increases in heat transfer above that existing for the fully frozen limit. In the catalytic combustor, suitable hot catalytic surfaces act as sources of atoms and radicals which diffuse towards the free stream combustion gases and maintain combustion at relatively low temperatures, thereby decreasing the production of NO_x and leading to a potential low-pollution combustor.

A species of interest in the combustion context is the hydrogen atom and the present work examines the heat transfer from shock tube dissociated hydrogen, in an argon thermal bath, to nickel and silicon dioxide surfaces. Previous work to determine the catalytic efficiency of various surfaces to hydrogen atom recombination [1] has been carried out in steady flow reaction tubes using hydrogen which had been dissociated by a radio frequency discharge. In the present work, hydrogen has been thermally dissociated by shock wave heating a hydrogen-argon mixture in a shock tube. This has permitted a study of surface recombination of atomic hydrogen at free-stream temperatures in the range from 2000 to 6000 K. Comparison of the results of absolute heat transfer measurements to flat plates with existing theoretical predictions has been made to examine the relevance of such methods to combustion applications. Relative heat-transfer measurements to adjacent nickel and silicon dioxide surfaces have resulted in new data for their catalytic efficiencies to hydrogen atom surface recombination.

2. HEAT TRANSFER IN CHEMICALLY REACTING LAMINAR BOUNDARY LAYERS

Fay and Riddell [2] and Lees [3] have formulated the boundary layer equations including the effects of chemical dissociation. They considered that heat is transferred to the wall by normal molecular conduction and in addition by diffusion of atoms which recombine, either in the gas phase, or on the wall. There are two extremes possible: a very fast recombination rate in which the gas is in equilibrium throughout the boundary layer, or chemically frozen flow where the atom concentration remains constant through the layer. For these extreme cases Lees simplified the boundary-layer equations and solved them approximately.

Fay and Riddell solved the equations numerically for all values of the recombination rate. Both Lees [3] and Fay and Riddell [2], however, assumed that the boundary layer condition at the wall was that the atom concentration is zero; this corresponds to an infinitely efficient catalyst.

Goulard [4] allowed for atom concentrations at the wall greater than zero and deduced that for equilibrium, the mass flux of atoms diffusing towards the wall must equal the rate of atom mass lost by recombination at the wall. He showed that for frozen boundary layers, the heat-transfer rate to a surface having a wall recombination rate k_w is given in terms of the heat-transfer rate to a perfectly catalytic surface ($k_w = \infty$) as:

$$\frac{\dot{q}_{k_w}}{\dot{q}_{k_w = \infty}} = 1 + \frac{Le^{2/3} \frac{\alpha_A h_A^0}{h_T}}{1 + (Le^{2/3} - 1) \frac{\alpha_A h_A^0}{h_T}} (\phi - 1) \quad (1)$$

where:

$$Le = \text{is the Lewis number} = \frac{\rho D \bar{c}_p}{K}$$

$\alpha_A h_A^0/h_T$ represents the chemical fraction of the stagnation enthalpy h_T , α_A is the free stream atom fraction,

$$\phi = \left[1 + \frac{S}{k_w} \right]^{-1} \quad (2)$$

D = diffusion coefficient,

\bar{c}_p = frozen specific heat,

K = thermal conductivity,

ρ = density,

S = boundary-layer diffusion rate,

$$\left(= \frac{c_f \sqrt{Re_x}}{2Pr_w^{2/3}} \frac{\rho_e}{\rho_w} \frac{U_e}{\sqrt{Re_x}} \right)$$

The criterion determining whether the boundary layer remains frozen is the gas phase Damkohler number. Chung [5] has shown that for a flat plate laminar boundary layer, the gas phase Damkohler number ζ_g is given by

$$\zeta_g = \frac{4x}{U_e} \frac{k_{R_0}}{T_e^{w+2}} \left[\frac{P}{R_0} \right]^2 = \frac{\tau_d}{\tau_r} \quad (3)$$

where:

τ_d is the characteristic boundary layer particle diffusion time,

τ_r is the characteristic reaction time,

$k_{R_0} = 2k_R T^w$,

k_R is specific recombination rate coefficient,

w is the exponent of temperature in the expression $k_R = A/T^w$,

R_0 is the universal gas constant,

P , T_e and U_e are the static pressure, temperature and velocity at the edge of the boundary layer respectively.

x is the longitudinal distance from the edge of the boundary layer.

If ζ_g is sufficiently small, atomic species will not recombine in the boundary layer and will diffuse to the surface. The extent of surface recombination is determined by the catalytic nature of the surface material and is characterized by a surface Damkohler number ζ_s , which has been defined by Chung [5] for a flat plate laminar boundary layer as

$$\zeta_s = \frac{Sc(\rho_w k_w) \sqrt{x}}{(\rho_e U_e \mu_e c/2)^{1/2}} = \frac{\tau_d}{\tau_w} \quad (4)$$

where:

τ_d = characteristic particle diffusion time,
 τ_w = characteristic time for surface reaction,
 Sc is the Schmidt number ($= Pr/Le$),
 k_w is the specific wall reaction rate

$$\left[= \gamma' \left(\frac{R_0 T}{2\pi M_A} \right)^{1/2} \right],$$

c is the ratio of the density viscosity product ($\rho\mu/\rho_e\mu_e$). Subscripts w and e refer to wall and boundary layer edge conditions respectively.

γ' is the surface catalytic efficiency,
 M_A is the molecular weight of the atomic species.
 Vidal [6] has shown that for flat plate laminar boundary layers

$$St\sqrt{Re_x} = \frac{c_f\sqrt{Re_x}}{2(Pr_w)^{2/3}} \left[1 + \frac{U_e^2/2}{(h_T - h_w)} (Pr_w^{1/2} - 1) - \frac{\alpha_A h_A^0}{(h_T - h_w)} (1 - \phi Le) \right] \quad (5)$$

where $\phi = (1 + S/k_w)^{-1}$ and the boundary layer diffusion rate S is defined in equation (2).

The stagnation enthalpy h_T is defined by

$$h_T = \bar{c}_p T_e + \frac{1}{2} U_e^2 + \alpha_A h_A^0.$$

The surface heat-transfer rate \dot{q} may be calculated using the Stanton number, St , from equation (5) using

$$\dot{q} = St\rho_e U_e (h_T - h_w). \quad (6)$$

For the purpose of comparison with the heat-transfer measurements of the experimental programme, heat-transfer calculations to flat surfaces have been made for (a) shock heated 10% H_2 /90% Ar mixtures and (b) pure argon as test gases.

For dissociated hydrogen/argon mixtures the heat-transfer rate was calculated using equation (5) with $c_f\sqrt{Re_x}$ evaluated using the method proposed by Vidal [6] for non-unit Prandtl number and variable density-viscosity product across the boundary layer. For the conditions of the present experiments, this leads to results for $c_f\sqrt{Re_x}$ within 1% of the classical Blasius laminar boundary layer result of 0.664.

Values of the relevant transport properties of the equilibrium hydrogen-argon mixture in the shocked gas zone such as viscosity, diffusivity and thermal

conductivity (shown in Figs. 1–3) were evaluated using the methods given in Appendix A at temperatures up to 6000 K, at which the hydrogen is fully dissociated. Computed values of the Reynolds (Re), Prandtl (Pr), Schmidt (Sc) and Lewis (Le) numbers, together with the boundary-layer diffusion rate S [defined by equation (2)], are shown in Fig. 4 over a range of temperature from approximately 2000 to 6000 K at an assumed initial shock tube pressure of 1 torr typical of the experimental conditions. The effects of the onset of hydrogen dissociation commence at temperatures in excess of 2000 K.

As a basis for comparison of the reacting gas heat-transfer measurements with those for an inert gas, experiments were performed over the same temperature range using pure argon as an inert test medium. Theoretical estimates of heat transfer from pure argon were made using equation (6) together with the assumption that argon behaved as a perfect gas with $c_p = 5R_0/2M_{Ar}$ over the range of temperature explored. The Stanton number, St , was calculated from

$$St\sqrt{Re_x} = 0.332 \frac{\sqrt{c^*}}{(Pr)^{2/3}}$$

where $c^* = \rho^*\mu^*/\rho_e\mu_e$ and conditions * are evaluated at the boundary layer intermediate enthalpy h^* which is given by

$$h^* = 0.5(h_e + h_w) + 0.22(h_r - h_e)$$

and h_r is the recovery enthalpy defined as

$$h_r = h_e + \frac{1}{2}(Pr)^{1/2} U_e^2.$$

Transport properties were calculated using the assumption that argon behaved as an ideal monatomic gas over the range of temperature considered. The experimental results suggest that this assumption is satisfied at temperatures up to approximately 5000 K but departures, probably caused by argon ionisation, occur above this temperature.

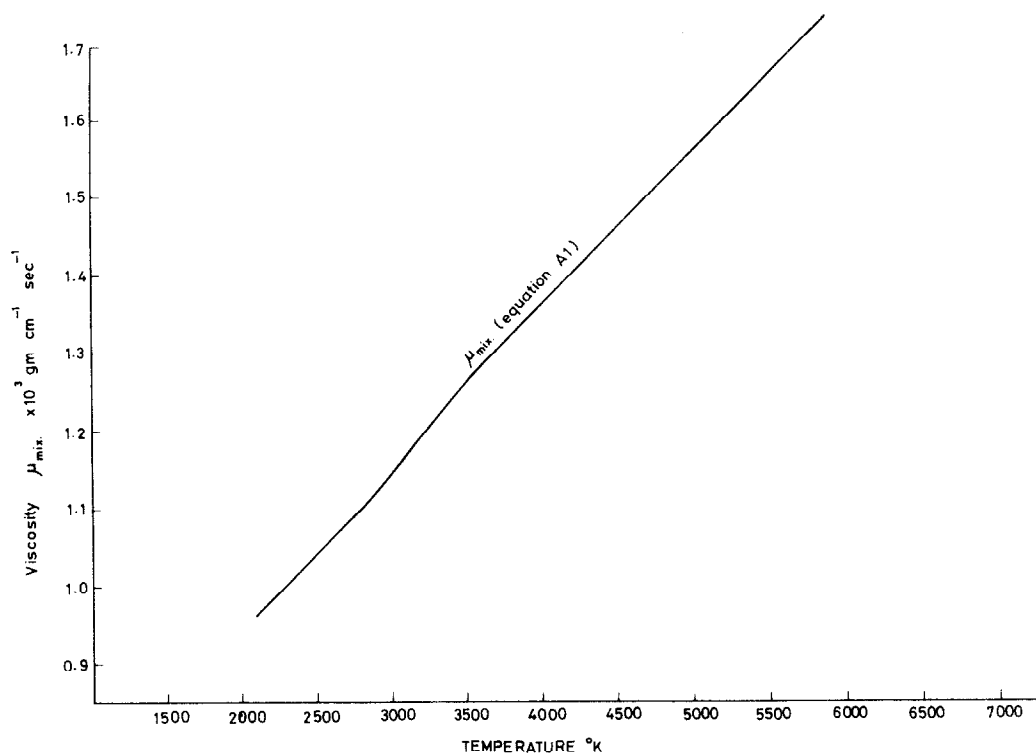
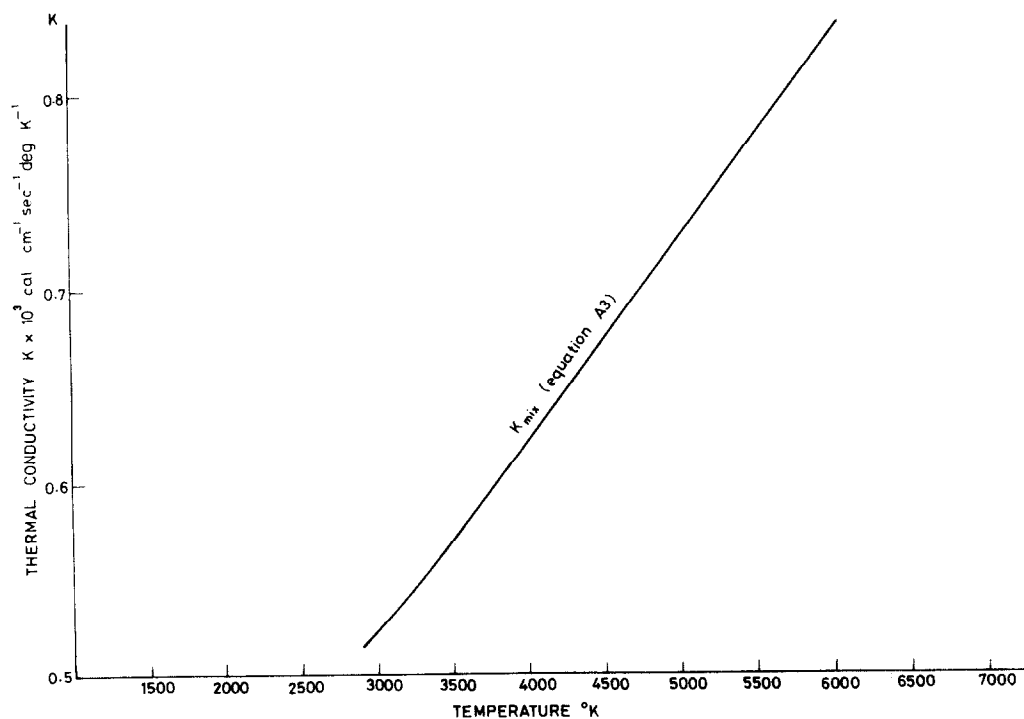
3. EXPERIMENTAL APPARATUS

3.1. The shock tube

The shock tube is a well-established technique to provide a dissociated flow and the atom concentration behind the incident shock front can be predicted with a high degree of confidence.

For the reported experiments a stainless steel shock tube has been used, having a 4.57 m long driver section and 12.75 m long driven section, both of 127 mm ID. Aluminium diaphragms, prescribed to ensure symmetrical opening, were allowed to burst naturally using cold hydrogen as a driver gas at pressures up to 40 bar. The channel or low pressure section of the tube was normally evacuated to about 10^{-3} torr with a combined leak and degassing rate of about 0.9×10^{-3} torr/min.

The shock detection system consisted of thin film platinum resistance gauges fitted to the shock tube wall. These gauges were mounted along the entire

FIG. 1. Viscosity of 10% H₂/90% Ar mixture at $p_1 = 1$ torr.FIG. 2. Thermal conductivity of 10% H₂/90% Ar mixture at $p_1 = 1$ torr.

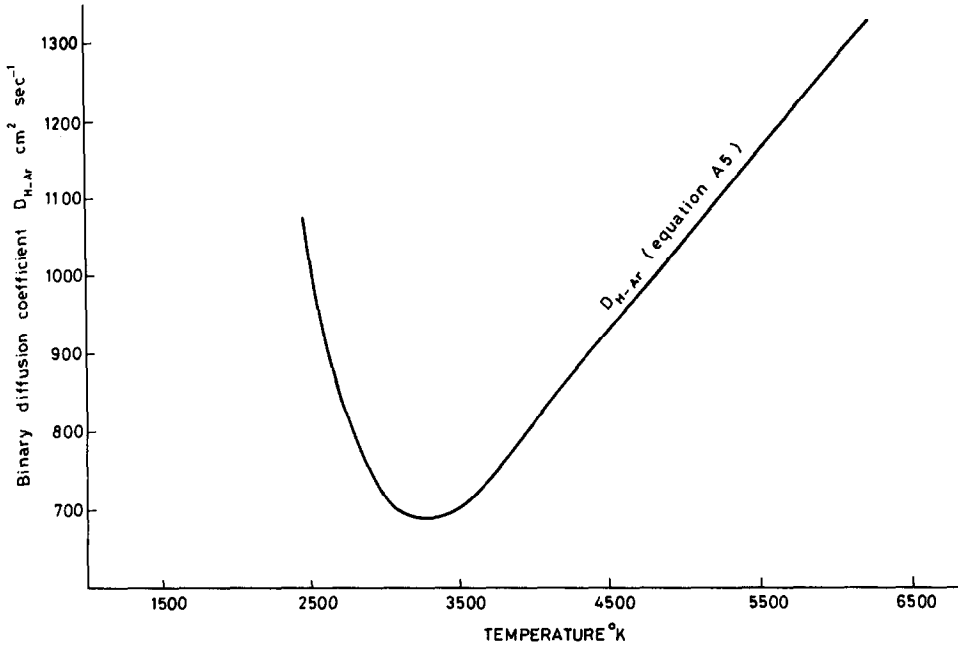


FIG. 3. Diffusion coefficient of hydrogen atoms in argon at post shock conditions ($p_1 = 1$ torr).

driven section at intervals of 1.22 m, giving a maximum of six shock detection locations. In addition, there were two further gauges at distances 1.05 m and 0.3 m from the location of the model. Signals from these detectors were passed through pulse amplifiers and recorded as

pulses on an oscilloscope raster display. The time makers were at $5 \mu\text{s}$ intervals and the time resolution of this recording system was approximately $1 \mu\text{s}$. This system permits the determination of the shock speed history ahead of the model.

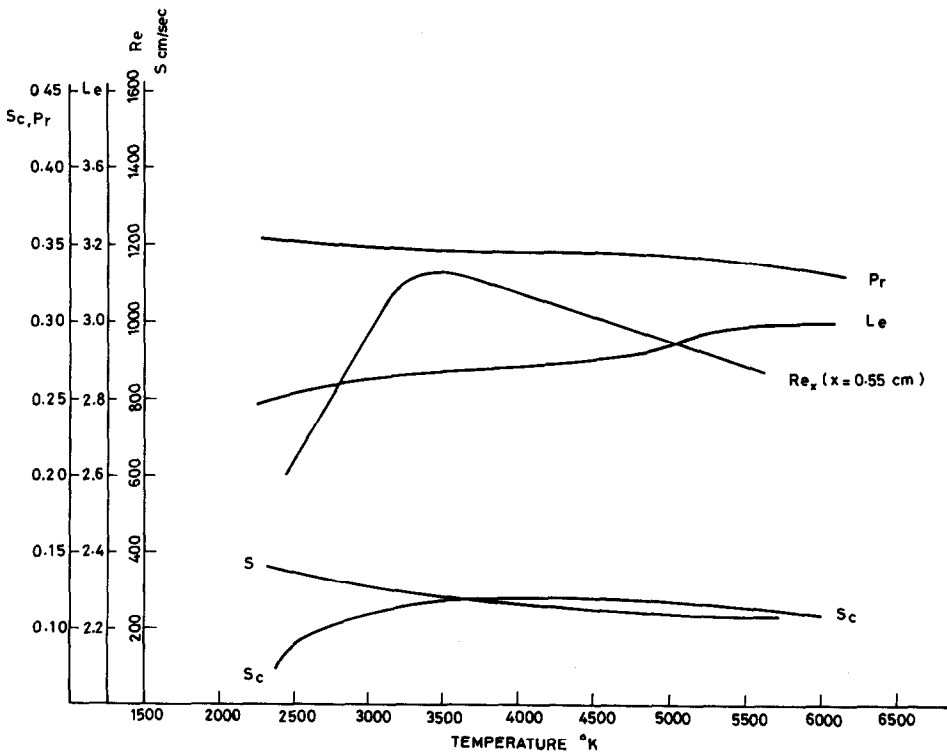


FIG. 4. Prandtl, Schmidt and Lewis numbers for 10% H_2 /90% Ar mixtures at post shock conditions ($p_1 = 1$ torr).

3.2. The heat transfer model

The basic scheme in surface catalysis experiments is to mount two adjacent heat-transfer gauges on a simple body. One gauge is coated with a relatively non-catalytic material - such as silicon dioxide - and measures the convective heat transfer together with a small contribution from surface recombination. The other gauge is coated with a material known to catalyse atom recombination and it measures the sum of the convective heat transfer and the heat released from atom recombination.

The model used for the present investigation is shown in Fig. 5 and consists of a flat plate made of Pyrex with three silver leads; two leads are along the sides and a middle one is used as a common lead. These leads were painted and fired in an oven at the yielding temperature of the Pyrex. A nickel film of 0.7 mm

width and 0.05 μm thickness was vacuum deposited, using a mask, on top of the plate. A covering layer of silicon monoxide (allowed to oxidise to SiO_2) of thickness 0.5 μm was also vacuum deposited on top of the gauge to act as a relatively non-catalytic layer for one gauge and a base on which to deposit a catalytic layer on the other. In the present investigation a 0.05 μm thickness of pure nickel has been used as a catalytic layer. The flat plate is 16 mm long and 5.7 mm wide and 2.2 mm thick. The flat plate has been mounted in the middle of the shock tube. Details of the construction and manufacture of the gauge may be found in [7]. The dimensions of the plate were chosen to ensure that the boundary-layer state was laminar for all of the experimental conditions investigated.

Measurements of the heat transfer were obtained in the usual manner using transient surface resistance

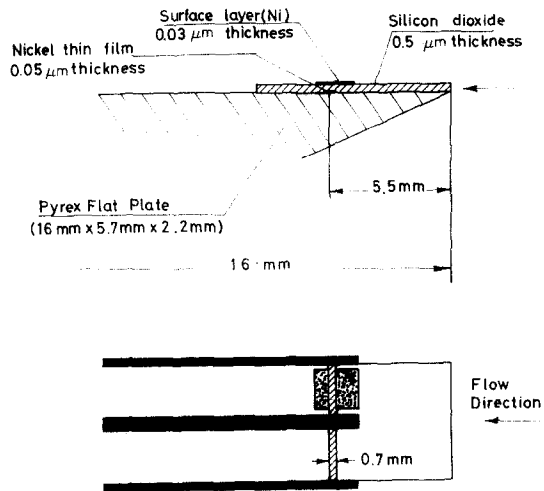


FIG. 5a. Flat plate dual catalytic/non-catalytic heat-transfer sensor.

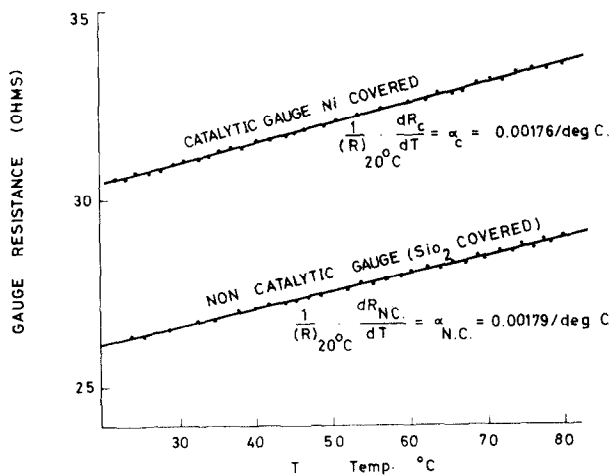


FIG. 5b. Gauge resistance variation with temperature.

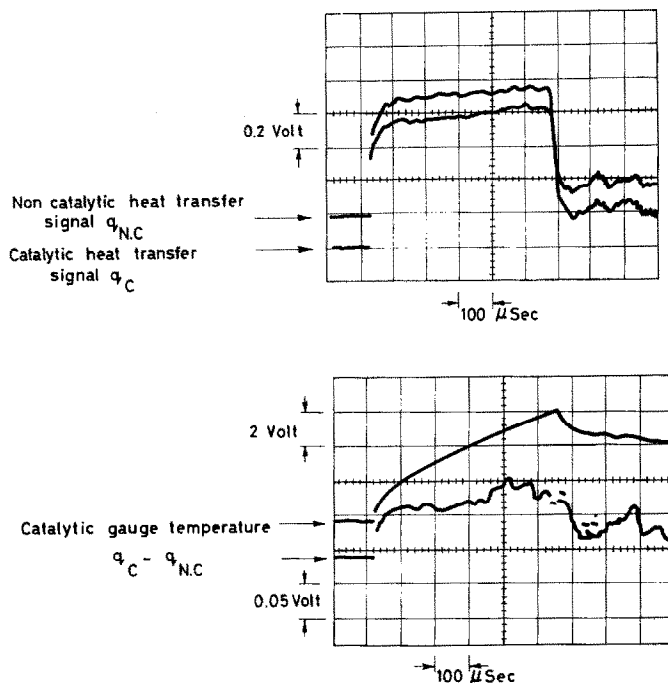


FIG. 6a. Typical heat-transfer records.

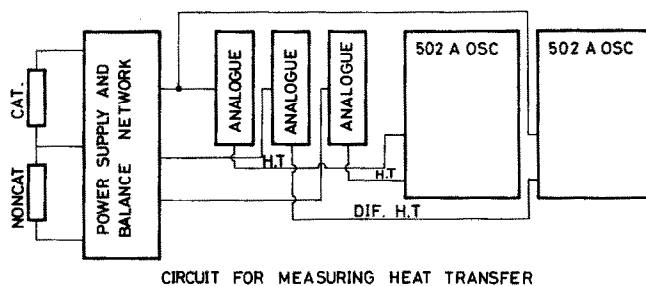


FIG. 6b. Block diagram of measuring circuit.

thermometry and T section analogue circuits. An independent method for calibrating the gauges has been used before and after the tests. Figure 5 shows the flat plate heat-transfer sensors and the variation of their resistance with temperature. Figure 6 shows typical heat-transfer records from the gauges and a block diagram of the measuring circuit.

4. EXPERIMENTAL SURFACE HEAT-TRANSFER RATE RESULTS AND DISCUSSION

The experimental programme has been carried out to investigate hydrogen atom recombination on nickel and silicon dioxide surfaces. The test gas, a 10% hydrogen/90% argon mixture by mole fraction, was mixed in a separate receiver for 1 h, at least, before using it in the shock tube. The transport properties of

the mixture have been calculated as described in Appendix A at estimated post shock conditions for an initial gas pressure of 1 torr and for a range of shock Mach numbers covering no dissociation to full dissociation limits. These calculations, summarised in Figs. 1-4 demonstrate the high values of Lewis number approaching 3.0 appropriate to the diffusion of hydrogen atoms as the gas mixture becomes more dissociated with increase of temperature.

In comparative heat-transfer experiments involving catalytic/non-catalytic surfaces, the accuracy of experimental observations is improved if the ratio of the chemical enthalpy potentially available from surface recombination to the stagnation enthalpy is as large as possible. For the chosen 10% H_2 /90% Ar mixture the chemical enthalpy fraction, shown in Fig. 7, reaches a

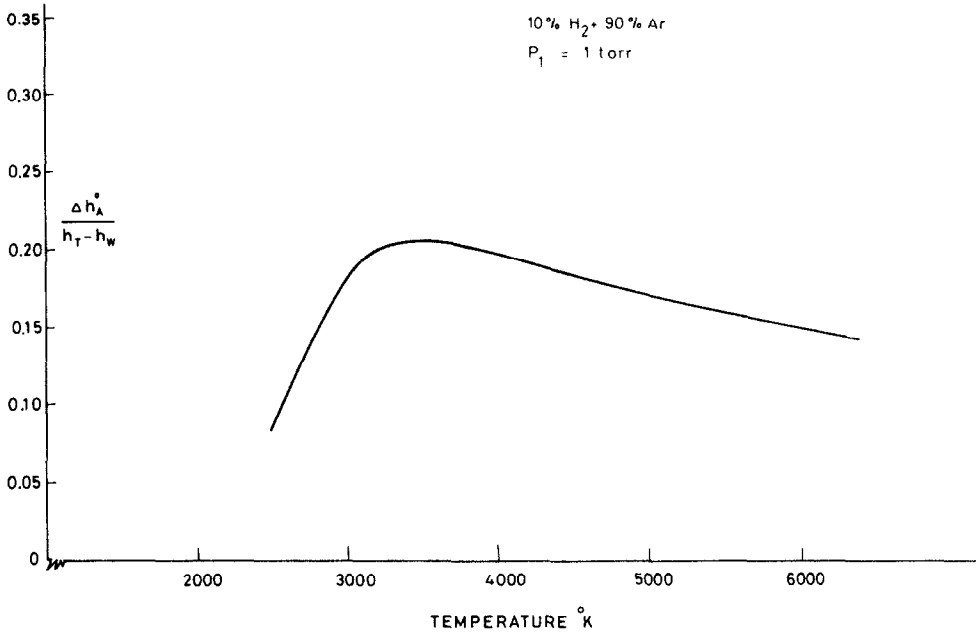


FIG. 7. Hydrogen dissociation energy fraction for 10% H₂/90% Ar mixture at p₁ = 1 torr.

maximum of about 0.20 at post shock conditions for an initial shock tube pressure of 1 torr. The results shown in Fig. 7 have been calculated using the data of [8] and assuming chemical equilibrium immediately downstream of the incident shock. At low temperatures the chemical enthalpy fraction is zero corresponding to no dissociation of the hydrogen. The fraction increases with temperature until the hydrogen is fully dissociated and then decreases as the total enthalpy increases with the chemical enthalpy con-

stant at its fully dissociated value. It would be expected that the available chemical enthalpy fraction would increase with increase in the hydrogen concentration in the mixture. However, in practice, the shock tube performance characteristic for a given driver gas limits the achievable chemical enthalpy fraction since the performance deteriorates as the hydrogen fraction increases.

Figure 8 shows the absolute heat-transfer measurements for both Ni and SiO₂ surfaces which are

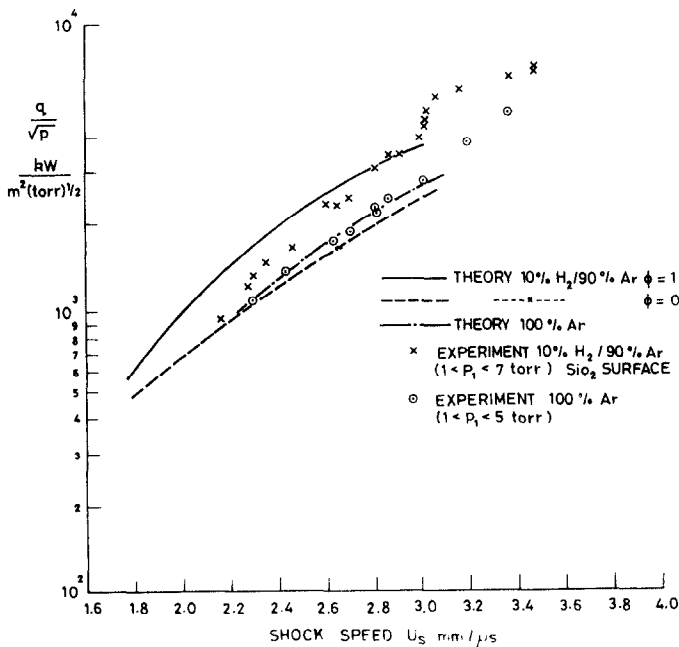


FIG. 8. Measured heat-transfer rates in pure argon and 10% H₂/90% Ar mixture.

compared with the predictions based on Vidal's theory [equation (5)] for the equilibrium ($\phi = 1$) and chemically frozen ($\phi = 0$) limits. The absolute values of the experimental data for both surfaces show best agreement with equilibrium predictions at values of shock speed U_s between 2.5 and 3.0 mm/ μ s, suggesting that even though the boundary-layer gas phase reactions are frozen, the surface reactions are near the equilibrium limit.

At low values of the shock speed ($U_s < 2.5$ mm/ μ s) it is possible that the shocked gas may not have reached equilibrium. Estimates of a characteristic dissociation relaxation time based on the following dissociation rate constant given by Baulch *et al.* [9] for the reaction $H_2 + Ar \rightarrow H + H + Ar$, $k_D = 2.20 \times 10^{11} \exp(-96000/1.987T)$ [$m^3/kg \text{ mole K}$], are shown in Fig. 9. Comparison is made between the characteristic time for 20% dissociation and the available test time in the shocked gas. It is concluded that the flow could still be non-equilibrium at shock speeds below 2.6 mm/ μ s.

At high shock speeds ($U_s > 3.0$ mm/ μ s) the heat-transfer measurements are higher than the theoretical prediction. However, much greater uncertainty exists

in the values of the transport properties used in the prediction and the lack of agreement in this experimental regime is attributed to this reason.

As a test of the absolute validity of the heat-transfer sensor calibrations comparisons were also made between theoretical heat-transfer predictions and the results of experiments using pure argon in the test medium. Excellent agreement is shown in Fig. 8 at values of shock speed up to $U_s = 3.0$ mm/ μ s. The departure between theory and experiment at greater shock speeds is likely to be a consequence of argon ionisation.

From the results summarized in Fig. 8 it is deduced that the nickel surface may be considered to be near the fully catalytic limit, whereas the silicon dioxide surface is partially catalytic to H atom recombination. Previously reported measurements by Wood *et al.* [10] of the catalytic efficiency (γ') of nickel surfaces to H atom recombinations resulted in a value of $\gamma' = 0.20$. This gives a value of ϕ_{Ni} [see equation (5)] of 0.982 for the present experimental conditions which would be reduced only to 0.965 even if the value of γ' was halved. Thus both the present results and previous work justify

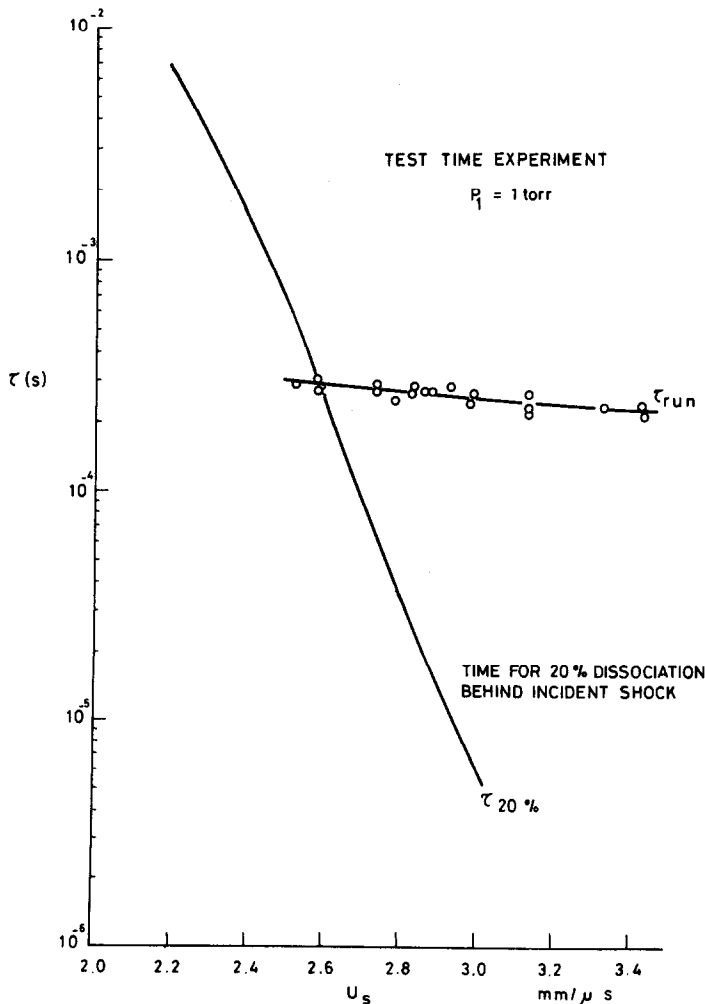


FIG. 9. Comparison of time for 20% dissociation with measured test time.

the assumption of the fully catalytic value of $\phi_{\text{Ni}} = 1.0$ in the subsequent analysis. Using this assumption and following Vidal's expression for surface heat transfer [equation (5)], the ratio of the heat transfer to the silicon dioxide and nickel surfaces is given by

$$\frac{\dot{q}_{\text{SiO}_2}}{\dot{q}_{\text{Ni}}} = \frac{\left[1 + (Pr_w^{1/2} - 1) \left(\frac{\frac{1}{2} U_e^2}{h_T - h_w} \right) - \left(\frac{\alpha_A h_A^0}{h_T - h_w} \right) (1 - \phi_{\text{SiO}_2} Le) \right]}{\left[1 + (Pr_w^{1/2} - 1) \left(\frac{\frac{1}{2} U_e^2}{h_T - h_w} \right) - \beta \left(\frac{\alpha_A h_A^0}{h_T - h_w} \right) (1 - Le) \right]} \quad (7)$$

where the energy accommodation β for H atom recombination on nickel surfaces is assumed to be 60% [10] and for silicon dioxide it is assumed to be unity. The conclusions from the experimental results are relatively insensitive to the value of β chosen for silicon dioxide surfaces, since $\dot{q}_{\text{SiO}_2}/\dot{q}_{\text{Ni}}$ is changed only by about 1% from the $\beta = 1.0$ value for an assumed β_{SiO_2} of 0.6 for $\phi_{\text{SiO}_2} = 0.4$. In view of the estimated experimental errors involved in the measurements of surface heat transfer, it is not anticipated that the effect of the variation of β_{SiO_2} could be resolved by the present experiments.

The measured variation of the ratio of the silicon dioxide heat transfer to the fully catalytic heat transfer to nickel surfaces is shown in Fig. 10. The experiments are compared with the predicted heat-transfer ratio using equation (7) for various assumed values of ϕ_{SiO_2} . The chemical enthalpy fraction $\alpha_A h_A^0/(h_T - h_w)$ was obtained from Fig. 7 assuming equilibrium flow downstream of the shock. The values of the Lewis number used in equation (7) were evaluated at post shock conditions and obtained from Fig. 4. Experimental results are also shown in Fig. 10 for catalytic

nickel surfaces which extended to the plate leading edge. Negligible differences in surface heat transfer were observed, thereby indicating the near fully catalytic behaviour of the nickel.

The comparison between experiment and theory

shown in Fig. 10 suggests that best agreement is given by a value of $\phi_{\text{SiO}_2} \approx 0.4$ for values of shock speed U_s in excess of 2.7 mm/ μ s. For lower shock speeds relatively less difference in heat transfer was measured which supports the conclusion of Figs. 8 and 9 that the shocked flow has probably not reached equilibrium with the consequence that less chemical enthalpy is available than predicted using equilibrium assumptions.

Using the best fit value of ϕ_{SiO_2} of 0.4, a value for the surface catalytic efficiency γ' of silicon dioxide to hydrogen atom recombination may be deduced since

$$\frac{S}{k_w} = \frac{1}{\phi} - 1$$

where k_w is the surface recombination rate and S is the boundary-layer diffusion rate given by

$$S = \frac{c_f \sqrt{Re_x}}{2Pr_w^{2/3}} \frac{\rho_e}{\rho_w} \frac{U_e}{\sqrt{Re_x}}$$

Over the temperature range of the best fit value of ϕ_{SiO_2} , the value of S is approximately 2.28 mm/s. Thus

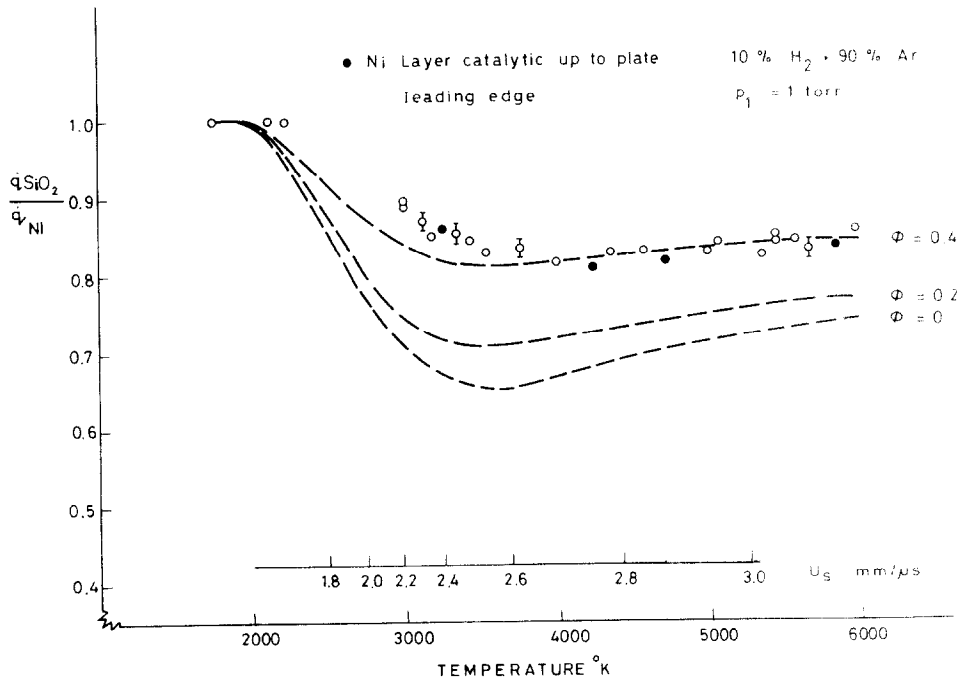


FIG. 10. Measured and calculated ratio of heat-transfer rates to nickel and silicon dioxide surfaces.

k_w is 5/1.5 or 1.52 m/s and the catalytic efficiency γ' is given by

$$\gamma' = k_w \left(\frac{2\pi M_H}{R_0 T_w} \right)^{1/2} = 24.5 \times 10^{-4}.$$

This value should be compared with a value of $\gamma' \approx 7.5 \times 10^{-4}$ for hydrogen atom surface recombination on Pyrex obtained by Wood, Mills and Wise [10] using a completely different experimental technique employing hydrogen atoms obtained by a radio frequency discharge.

5. CONCLUDING REMARKS

The reported experiments have shown that for nickel surfaces the heat-transfer rate from shock heated hydrogen/argon mixtures is close to the fully catalytic limit prediction. This is consistent with the rapid diffusion rates of hydrogen atoms together with the high surface recombination rates on metallic surfaces. Comparison of heat-transfer measurements on adjacent silicon dioxide and nickel surfaces, using the assumption that nickel is fully catalytic, has yielded a value of the catalytic efficiency (γ') for silicon dioxide to hydrogen atom surface recombination of approximately 25×10^{-4} . The value is consistent in order of magnitude with earlier measurements of the catalytic efficiency of Pyrex surfaces to H atom recombination by Wood and Wise [1] using a quite different experimental technique.

Acknowledgements – The authors wish to acknowledge the interest and the encouragement of Professor G. M. Lilley and useful discussions with Professor K. N. C. Bray.

REFERENCES

1. B. J. Wood and H. Wise, The kinetics of hydrogen atom recombination on Pyrex glass and fused quartz, *J. phys. Chem.* **66**, 1049–(1962).
2. J. A. Fay and F. R. Riddell, Theory of stagnation point heat transfer in dissociated air, *J. aeronaut. Sci.* **25**, 73 (1958).
3. L. Lees, Laminar heat transfer over blunt-nosed bodies at hypersonic flight speeds, *Jet Propul.* **26**, 259 (1956).
4. R. J. Goulard, Stagnation heat transfer, *Jet Propul.* **28**, 737 (1958).
5. P. M. Chung, Chemically reacting non-equilibrium boundary layer, *Advances in Heat Transfer*, Vol. II, pp. 109–270. Academic Press, New York (1965).
6. R. I. Vidal, Species diffusion in the frozen laminar boundary layer on a catalytic flat plate, AEDC-TR-67-88 (1967).
7. B. J. McCaffrey, R. A. East and M. W. Stent, A thin film catalytic-non-catalytic heat transfer gauge for shock tube measurements in reacting gases, AASU Report No. 336, University of Southampton (1976).
8. R. A. Svehla, Thermodynamic and transport properties for the hydrogen oxygen system, NASA SP 3011 (1964).
9. D. L. Baulch, D. D. Drysdale, D. G. Horne and A. C. Lloyd, Evaluated kinetic data for high temperature reactions, Vol. 1. Butterworths, London (1972).
10. B. J. Wood, J. S. Mills and H. Wise, Energy accommodation in exothermic heterogeneous catalytic reactions, *J. phys. Chem.* **67**, 1462 (1963).
11. J. O. Hirschfelder, C. F. Curtiss and R. B. Bird, *Molecular Theory of Gases and Liquids*. John Wiley, New York (1954).
12. C. R. Wilkie, A viscosity equation for gas mixtures, *J. chem. Phys.* **18**, 517–522 (1950).
13. E. A. Mason and S. C. Saxena, Approximate formula for the thermal conductivity of gas mixtures, *Physics Fluids* **1**, 361–369 (1958).
14. W. H. Dorrance, *Viscous Hypersonic Flow*. McGraw-Hill, New York (1962).

APPENDIX A

Transport properties of dilute gas mixtures

In order to use the predictions of theory for comparison with experimental results, the relevant transport properties of the hydrogen/argon mixture were required. The methods used for their calculation were as follows:

Coefficient of viscosity (μ). For a mixture of gases containing v components, Wilkie [12] has given the following mixture rule

$$\mu = \sum_{i=1}^v \mu_i \left(1 + \sum_{\substack{k=1 \\ k \neq i}}^v G_{ik} \frac{x_k}{x_i} \right)^{-1} \quad (\text{A1})$$

where:

μ_i is the viscosity coefficient of species i ,
 x_i is the mole fraction of species i ,

$$G_{ik} = \frac{[1 + (\mu_i/\mu_k)^{1/2} (M_k/M_i)^{1/4}]^2}{2^{3/2} [1 + (M_i/M_k)]^{1/2}}. \quad (\text{A2})$$

The viscosity coefficients for the gases in the pure state have been calculated using the following results of Chapman–Enskog theory described in [11]:

$$\mu_i = 266.93 \times 10^{-7} \frac{(M_i T)^{1/2}}{\sigma^2 \Omega^{(2,2)*}}$$

where:

μ_i = viscosity coefficient of species i , (gm/cm²·s),
 σ = collision diameter (Å),

$\Omega^{(2,2)*}$ = collision integral tabulated in [11].

Thermal conductivity (K). For a mixture of monatomic gases Mason and Saxena [13] have shown that

$$K = \sum_{i=1}^v K_i \left(1 + 1.065 \sum_{\substack{k=1 \\ k \neq i}}^v G_{ik} \frac{x_k}{x_i} \right)^{-1} \quad (\text{A3})$$

where the thermal conductivity of the monatomic gas of species i is given by the Chapman–Enskog result of

$$K_i = \frac{15}{4} \frac{R_0}{M_i} \mu_i. \quad (\text{A4})$$

Mason and Saxena have also shown that their mixture expression may be applied to polyatomic gases providing the pure gas thermal conductivities K_i are multiplied by a correction factor of $0.115 + (0.354 c_{pi} M_i / R_0)$ before use in the mixture rule of equation (A3).

Binary diffusion coefficient (D_{12}). The binary diffusion coefficient for hydrogen in argon has been calculated using the approximate expression given by Hirschfelder, Curtiss and Bird [11] based on a Lennard–Jones potential model:

$$D_{12} = D_{21} = 262.8 \times 10^{-5} \frac{[T^3 (M_1 + M_2) / 2 M_1 M_2]^{1/2}}{p \sigma_{12}^2 \Omega^{(1,1)*} (T_{12}^*)} \quad (\text{A5})$$

where:

$D_{12} = D_{21}$ = diffusion coefficient (cm²/s),
 p = pressure (bar),

$\sigma_{12} = \frac{1}{2}(\sigma_1 + \sigma_2)$ = mean collision diameter (Å),
 $\Omega^{(1,1)*}$ is the collision integral tabulated in [11] as a function of the reduced temperature T_{*2} where $T_{*2} = T/(\varepsilon_{12}/k)$ and $\varepsilon_{12} = \sqrt{\varepsilon_1 \varepsilon_2}$ is the mean depth of the potential well in the Lennard-Jones potentials for the two gases 1 and 2.

Calculations based on these equations have been performed for an initial mixture of 10% H₂ + 90% Ar by mole fraction ahead of the shock wave at an initial pressure of 1 torr. The results, which assume thermal and chemical equilibrium at the post shock conditions are shown in Figs. 1-3. The molecular data used have been obtained from [11] and [14] and are given in Table 1.

Table 1

Gas	σ (Å)	$\Omega^{(2,2)*}$	ε/k (K)
Argon	3.418	0.69	124
Hydrogen atom	0.657	4.5	52400
Equilibrium hydrogen argon mixture	2.037	1.175	2549

ETUDE PAR TUBE A CHOC DU TRANSFERT THERMIQUE ENTRE L'HYDROGENE DISSOCIE ET DES SURFACES CATALYTIQUES

Résumé — Des expériences avec un tube à choc permettent la comparaison des transferts thermiques entre des surfaces planes de nickel et de dioxyde de silice et des mélanges hydrogène/argon à des températures comprises entre 2000 et 6000 K. Les conditions expérimentales sont choisies de façon à permettre l'étude des effets sur le flux thermique de la recombinaison en surface des atomes d'hydrogène. On présente des comparaisons entre les expériences et les prévisions théoriques basées sur les méthodes connues de la couche limite. Les résultats fournissent une valeur expérimentale de l'efficacité catalytique (γ') des surfaces de dioxyde de silice vis-à-vis de la recombinaison des atomes d'hydrogène, soit 25×10^{-4} .

UNTERSUCHUNG DES WÄRMEÜBERGANGS VON DISSOZIIERTEM WASSERSTOFF AN KATALYTISCHE OBERFLÄCHEN IN EINEM STOßWELLENROHR

Zusammenfassung — Stoßwellenrohr-Versuche werden beschrieben, die den Wärmeübergang an die Oberfläche ebener Platten aus Nickel- und Silikondioxid von einem Wasserstoff-Argon-Gemisch bei Temperaturen zwischen 2000K und 6000K vergleichen. Die Versuchsbedingungen wurden so gewählt, daß die Einflüsse der Oberflächenrekombination der Wasserstoffatome auf die Größe des Wärmeübergangs untersucht werden konnten. Vergleiche zwischen den Versuchen und den theoretischen Voraussagen, die sich auf die bestehenden laminaren Grenzschichtmethoden stützen, wurden angestellt. Die Interpretation der Ergebnisse ergibt bei den Silikondioxid-Oberflächen einen experimentellen Wert von 25×10^{-4} für den katalytischen Nutzeffekt (γ') der Rekombination der Wasserstoffatome.

ИССЛЕДОВАНИЕ ТЕПЛОБМЕНА ДИССОЦИИРОВАННОГО ВОДОРОДА С КАТАЛИТИЧЕСКИМИ ПОВЕРХНОСТЯМИ В УДАРНОЙ ТРУБЕ

Аннотация — На установке с ударной трубой проведено сравнение между интенсивностью теплопереноса от смесей диссоциированного водорода с аргоном к плоским пластинам из никеля и двуокиси кремния в диапазоне температур от 2000 К до 6000 К. Экспериментальные условия подобраны таким образом, чтобы обеспечить возможность исследования влияния поверхностной рекомбинации атомов водорода на интенсивность теплообмена. Проведено сравнение экспериментальных данных с результатами теоретических расчетов ламинарного пограничного слоя. Путем обработки экспериментальных данных можно получить значение каталитической эффективности (γ') поверхностей из двуокиси кремния по отношению к рекомбинации атомов водорода порядка 25×10^{-4} .